Atmospheric Electric Propulsion Mission Performance Tool

Scott T. King* and Mitchell L. R. Walker†
Georgia Institute of Technology, Atlanta, Georgia 30332
and
Silvio G. Chianese‡
Northrop Grumman Corporation, Redondo Beach, California 90278

DOI: 10.2514/1.A32235

The amount of available propellant limits low-Earth orbit satellite lifetime due to the necessity of drag makeup. An electric propulsion device that uses in situ ions as propellants is considered as an alternative method for satellite drag makeup. This work presents a tool that consists of a one-dimensional thruster mathematical model integrated with the NASA International Reference Ionosphere to provide ion and neutral species densities for an electrostatic electric propulsion approach. This mathematical model predicts thrust, drag, and thruster power. The thrust-to-drag ratio and thruster power are averaged over the entire mission duration of one year and compared with various circular orbits and satellite configurations: 300–1000 km orbit altitude, 0–60 deg orbit inclination, low to high solar activity, 0.1–5.0 m^2 satellite frontal area, 1–10 kV acceleration voltage, and 1–10 m^2 total grid area. The Satellite Tool Kit provides orbit propagation. An average thrust-to-drag ratio greater than one is achievable for many thruster and orbit configurations considered in this analysis, at power levels less than 90 W. Most satellite missions at altitudes of less than 400 km may fall into the region in which the thrust-to-drag ratio is less than one. Thrust-to-drag ratio values of less than one will still benefit satellites by extending mission lifetimes for months or years with average power requirements less than 100 W.

Nomenclature

A_{grid}	=	physical grid area, m^2
A_{open}	=	open grid area, m^2
$A_{s/c}$	=	spacecraft frontal area, m^2
C_D	=	coefficient of drag
D	=	total drag, N
D_{grid}	=	drag due to thruster, N
D_i	=	drag due to ions, N
D_{neut}	=	drag due to neutral species, N
$D_{s/c}$	=	drag due to spacecraft, N
E_i	=	first ionization energy of species i, eV
j_i	=	current density of species i, A/m^2
m_i	=	mass of species i, kg
$\dot{m}_i$	=	mass flow rate of species i, kg/s
$\dot{m}_i''$	=	mass flow rate of species i per unit area, $kg/s/m^2$
n_i	=	number density of species i, particles/m^3
P_{elec}	=	total electrical power, W
P_{grid}	=	grid power, W
P_{ion}	=	ionization power, W
P_{jet}	=	jet power, W
q	=	elementary charge unit, C
T	=	total thrust, N
v_{in}	=	inlet velocity, m/s
$v_{\text{out},i}$	=	exit velocity of species i, m/s
$v_{s/c}$	=	spacecraft orbital velocity (with respect to Earth), m/s
x_{loss}	=	loss factor of ion potential raising device
Z	=	charge state
ΔV	=	total acceleration voltage, V
ρ_{atmo}	=	atmospheric density, kg/m^3
ρ_i	=	density of species i, kg/m^3

Presented as Paper 2011-6000 at the 47th Joint Propulsion Conference & Exhibit, San Diego, CA, 31 July–3 August 2011; received 27 June 2012; revision received 1 June 2013; accepted for publication 5 June 2013; published online 14 February 2014.

*Graduate Research Assistant, School of Aerospace Engineering; scott.king@gatech.edu. Student Member AIAA.

†Associate Professor, School of Aerospace Engineering; mitchell.walker@ae.gatech.edu. Associate Fellow AIAA.

‡Northrop Grumman Aerospace Systems; currently Propulsion Development Engineer, Space Exploration Technologies, Hawthorne, CA 90250; silvio.chianese@spacex.com. Senior Member AIAA.

I. Introduction

SATELLITE missions in low-Earth orbit, which allow communication, science, and detection of natural threats, are heavily constrained by the lifetime of the satellite. A major factor in the determination of the satellite lifetime is the amount of propellant available to make up losses from the atmospheric drag during mission operations.

The ionosphere, the region in which near-Earth satellites orbit, contains many different particles, including neutral atoms, ions, and electrons. Dressler showed in [1] that electric propulsion (EP) could provide propulsive power to Earth-orbiting satellites through the acceleration of ions in the ionosphere. Figure 1 shows the design of an ambient atmosphere ion thruster (AAIT) that uses two grids supplied with different electric potentials to create an acceleration region for positively charged ions. This electrostatic EP approach in [2] creates thrust and counteracts drag losses as the satellite orbits Earth. It is important to note that this electrostatic approach is not physically realizable with the given design. The potential of incoming ions must be raised so that the difference between the raised ion potential and the space potential causes acceleration. At altitudes as low as 300 km, the ratio of neutral atoms to ions is large, up to a value of several hundred, which means that ions can be created in regions of high potential, relative to ambient space potential, by electron bombardment, arc discharges, radio frequency heating, or microwave heating then subsequently accelerated electrostatically. At altitudes up to 900 km, the ratio of neutral atoms to ions is typically on the order of 1, which is much lower than the ratio at lower altitudes. In this case, one may still create ions in a region of high potential and accelerate those ions electrostatically, or one may choose another acceleration method such as a linear particle accelerator. There are many possible manifestations of these methods, and the development of such an ion potential raising device is beyond the scope of this paper; therefore, ionization power estimates are calculated based on the first ionization energy of each incoming particle. Therefore, this study tests an atmospheric EP tool and examines the feasibility of such an electrostatic device with an estimate of the ionization energy costs. The AAIT allows future satellites to orbit longer than current

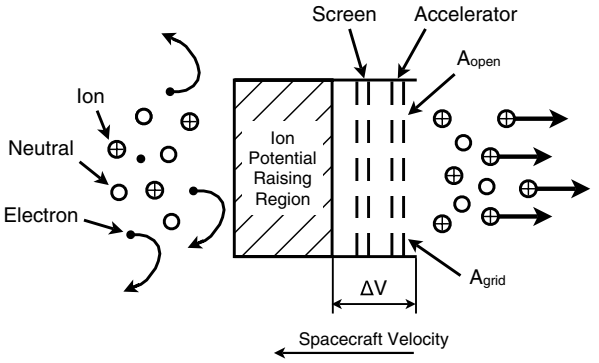

Fig. 1 AAIT concept with ion potential raising, ion acceleration, electron repulsion, and neutral transparency.

satellites that use limited onboard propellant by using in situ ions as propellants.

The design of an atmospheric EP device requires knowledge of the species densities of the ionosphere and a detailed mathematical model that uses this atmospheric data. The Atmospheric EP Mission Performance Tool (AEPMPT) developed during the design of the AAIT is unique. The tool integrates an electrostatic EP mathematical model with an atmospheric model to obtain ion densities during specific orbits and predict thruster performance. More importantly, the tool is not limited to an electrostatic EP approach; users of the code may alter the mathematical model to include other acceleration mechanisms and accommodate specific thruster configurations. The following sections describe the development, assumptions, and results of the mathematical model.

II. Mathematical Model and Assumptions

The AAIT uses the same electrostatic acceleration principles as a gridded ion engine. Figure 1 shows that positively charged particles are accelerated by an electric field created between two biased grids (screen and accelerator) to produce thrust [3]. The AAIT concept is unique because it claims to not require a discharge chamber. As the spacecraft orbits, the AAIT intercepts and accelerates ambient ions in the Earth's ionosphere.

The mathematical model is a one-dimensional model. It does not consider spatial variance normal to the AAIT grid plane; it assumes incoming ion velocity opposite the direction of the spacecraft velocity. The model calculates accelerated ion velocities using the conservation of energy (kinetic and electrostatic energies); thus, grid spacing is not considered. The model further assumes a constant number density over the entire AAIT grid area.

The following subsections describe the assumptions of each stage of the AAIT model and design. An atmospheric model is given, which identifies the ion, electron, and neutral atom number densities used for the thrust and drag predictions. These subsections also explain the mathematical formulation that underlies the thrust and drag calculations.

The goal of the AAIT performance code is to predict AAIT performance parameters from specific missions (various orbital parameters, each with a one year duration) with the corresponding ion densities for the associated orbits. The Atmospheric EP Mission Performance Tool integrates the Satellite Tool Kit (STK) of Analytical Graphics, Inc. to propagate specific orbits to obtain orbital parameters (time, altitude, latitude, and longitude), the NASA International Reference Ionosphere (IRI) 2007 [4–6] to calculate ion densities with the specific orbital parameters from STK, and the AAIT performance code. Thrust, drag, and power equations are defined explicitly in terms of inputs (ionosphere and satellite properties) the AAIT may experience in orbit.

A. IRI and STK Integration

The IRI is a detailed atmospheric model that provides electron temperature, electron density, and ion densities (O^+, H^+, He^+, O_2^+, NO^+, and N^+) as functions of year, month, day, hour, latitude, longitude, and altitude.

The AEPMPT integrates the IRI FORTRAN 77 files with a mathematical model to predict the AAIT performance. STK propagates selected orbits, and the output data provide atmospheric density and orbital parameters (time, altitude, latitude, and longitude) to obtain ion densities from the IRI.

Integrating the IRI with STK output data reduces uncertainty due to the rounding and interpolation of orbital data. Integration allows the use of the exact time, height, latitude, and longitude in the IRI without requiring any rounding, for example, to the nearest 10 deg, 10 km, or 15 min. Moreover, the only estimated data in this analysis, aside from the mathematical model, includes the IRI model estimates of the electron and ion number densities. The IRI assumes quasi neutrality and calculates the ion number density as a percentage of the electron number density [6].

Figure 2 shows the flow chart of the Atmospheric EP Mission Performance Tool. The first loop reads through all the selected STK output files to store the orbital data required for IRI execution. A second loop iterates through this orbital data to extract the electron density, electron temperature, and ion density from the IRI at each STK orbit propagation point. In this analysis, the orbit propagation points are approximately every 60 s.

A third loop runs through all of the selected orbits and calculates thrust, drag, and power. This can be a large amount of data points (a year-long orbit contains approximately 525,000 propagation points at 60 s intervals); therefore, average values are calculated for each orbit for a simple comparison of any orbits of interest.

B. Thrust Calculation

Equation (1) shows the thrust calculation as a momentum change caused by ion acceleration:

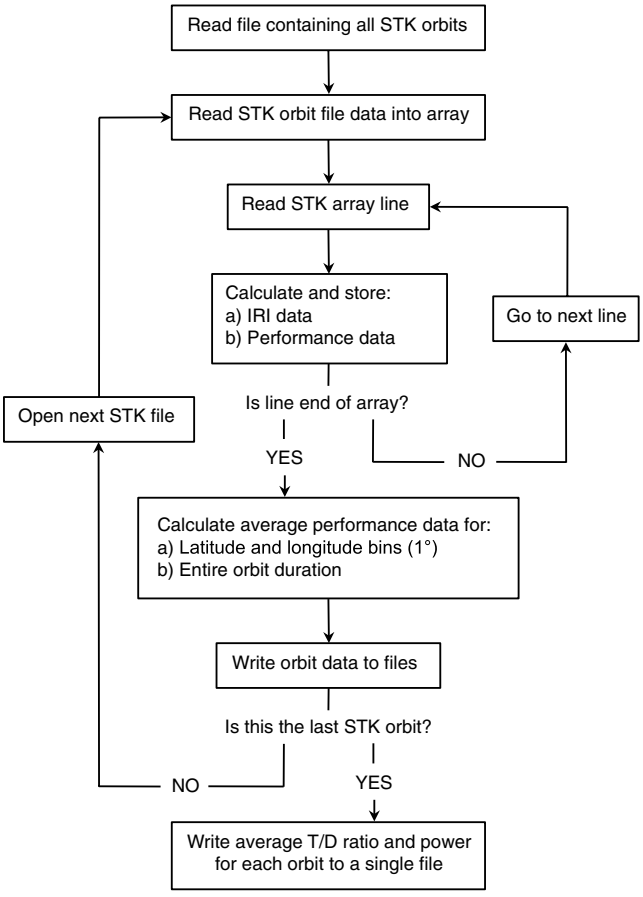

Fig. 2 AEPMPT path including nested loops, IRI integration, and data output.

$$T = \sum_i T_i = \sum_i \dot{m}_i(v_{\text{out},i} - v_{\text{in}}) = \sum_i \dot{m}_i'' A_{\text{open}}(v_{\text{out},i} - v_{\text{in}}) \tag{1}$$

The speed of the incoming particles v_{in} is assumed to be identical to the spacecraft orbital speed $v_{s/c}$ in a fixed-spacecraft frame of reference. The spacecraft velocity is obtained from orbit analysis in the STK. The grid transparency, defined as the percentage of the open area to the total grid area, is set as a constant in this analysis at 90%.

Each species is considered independently, as each ion species has not only a different mass flux but also a different exit velocity achieved from the potential difference between the ion potential and ambient space potential. From energy conservation, the energy transferred to an ion is equal to the product of the charge and the potential difference. The exit velocity of each ion species results from this conservation equation:

$$v_{\text{out},i} = \sqrt{\frac{2Zq\Delta V}{m_i}} \tag{2}$$

Equation (2) includes the charge state of the ion Z (assumed to be 1 for a singly charged state), the elementary charge value q, the acceleration voltage ΔV, and the mass of the ion m_i. Additionally, Eq. (2) assumes a purely axial motion.

The mass flow rate per unit area of each species is found by a comparative continuum fluid mechanics equation. Equation (3) provides the development of the particle density. In a rarified flow, more appropriate variables such as the number density n_i and particle mass replace the density term:

$$\dot{m}_i'' = \rho_i v_{\text{in}} = m_i n_i v_{s/c} \tag{3}$$

The total thrust is the contribution of the thrust from each incoming ion type (O^+, H^+, He^+, O_2^+, N^+, NO^+, and e^-). Electron repulsion is included here and represented by a negative contribution to the thrust since electrons may be repelled upstream by the relative negative bias of the screen grid.

C. Drag Calculation

The AEPMPT is combined with a drag model in a rarefied flow. Since the spacecraft orbits between 300 and 1,000 km, the atmosphere must be treated as a collection of individual particles. Therefore, the mass flux (mass per unit time per unit area) of each entering species is calculated independently and used in a sum of drag forces. The total drag is calculated by determining the drag due to each incoming species striking the spacecraft and summing each contribution:

$$D = D_{\text{neut}} + \sum_i D_i = (1/2)Av_{s/c}C_D\left(\rho_{\text{atmo}} v_{s/c} + \sum_i \dot{m}_i''\right) \tag{4}$$

Equation (4) shows that the drag is a function of the spacecraft velocity $v_{s/c}$, a reference drag area A, the coefficient of drag C_D, and the atmospheric density, which does not include ion number densities. The value of C_D used in these simulations is 2.4 [7,8]. Ions and neutral particles are considered separately in these calculations because STK exports only the neutral number density from the orbit simulation, and the IRI exports ion and electron number densities. The drag is due to both the spacecraft frontal area and the grid area with reference drag areas of $A_{s/c}$ and A_{grid}, respectively.

Both the spacecraft and the thruster use the same incoming ion velocity v_{in}, which is equal in magnitude to and opposite in direction of the spacecraft velocity. It is assumed that thermal motions are small relative to the spacecraft velocity and are neglected in this analysis. The drag due to electrons is included in the spacecraft drag term; however, the impact of electrons on the thruster momentum is captured in the thrust.

D. Power Requirement

An EP device requires a specific input electrical power to produce a given thrust, and these power requirements must be analyzed for practical AAIT use. All power estimations assume an efficiency of 100% unless noted otherwise. The thruster electrical power is a combination of three effects: 1) ions accelerated through the grids into the plume P_{jet}, 2) ions striking the grids P_{grid}, and 3) ion potential raising P_{ion}. Equation (5) shows the thruster power as a function of these three effects:

$$P_{\text{elec}} = P_{\text{jet}} + P_{\text{grid}} + P_{\text{ion}} = \sum_i (P_{\text{jet},i} + P_{\text{grid},i} + P_{\text{ion},i}) \tag{5}$$

Jet power, or beam power, is calculated with Eq. (6) using the current density passing through the grids j_i and the charge state of the ions Z:

$$\begin{aligned} P_{\text{jet},i} &= (1/2)\dot{m}_i v_{\text{exit},i}^2 = (1/2)\dot{m}_i'' A_{\text{open}}(v_{\text{out},i} - v_{s/c})^2 \\ &= j_i A_{\text{open}} \Delta V, \quad j_i = n_i v_{s/c} Zq = (\dot{m}_i''/m_i)Zq \end{aligned} \tag{6}$$

The grid power is calculated with Eq. (7) using the current density, the screen grid bias V_{screen}, and the physical area of the screen grid:

$$P_{\text{grid},i} = j_i A_{\text{grid}} V_{\text{screen}}, \quad j_i = n_i v_{s/c} Zq = (\dot{m}_i''/m_i)Zq \tag{7}$$

The ionization power is calculated with Eq. (8) using the mass flux, first ionization energy cost E_i, open area of the grids, and a factor x_{loss} to estimate power losses for a generic potential raising device. In this analysis, x_{loss} has been set to 10, which assumes that the potential raising device requires 10 times more power than the ionization power of all particles. Ionization energy is typically given in units of electron volts, so a conversion from electron volts to Joules is used: 1.6×10^{-19} J/eV. Ionization energies used in this calculation include 13.5984 eV for monatomic hydrogen (H), 24.5874 eV for helium (He), 14.5341 eV for monatomic nitrogen (N), 13.6181 eV for monatomic oxygen (O), 15.7596 eV for argon (Ar) [9], 9.2642 eV for nitric oxide (NO) [10], and 12.0697 eV for diatomic oxygen (O_2) [11]:

$$P_{\text{ion},i} = x_{\text{loss}} E_i (\dot{m}_i''/m_i) A_{\text{open}} \tag{8}$$

III. Atmospheric EP Mission Performance Tool Results

STK input files to the AEPMPT include orbit files with defining criteria such as the altitude, inclination, solar activity level (orbit year), and orbit duration. To test the performance tool and identify trends in AAIT performance, the orbit and satellite conditions include minimum and maximum values with a given number of steps. Table 1 lists all of the orbit, satellite, and AAIT configurations considered in this analysis. For example, the mission duration for this analysis is one year. Orbit altitude includes orbits from 300 to 1000 km in 100 km intervals. The solar activity level includes the solar maximum, solar mean, and solar minimum years, corresponding to 1991, 1993, and 1996 [12]. The AAIT acceleration voltage includes 1, 5, and 10 kV, as they represent the simplest design and indicate how

Table 1 AAIT, spacecraft, and orbital parameters varied in the analysis

Parameter	Values		
	Minimum	Interval	Maximum
Altitude, km	300	100	1000
Inclination, deg	0	30	60
	Minimum	Mean	Maximum
Solar activity level, year	1996	1993	1991
Satellite frontal area, m^2	0.1	1.5	5.0
AAIT total grid area, m^2	1	5	10
AAIT acceleration voltage, V	1000	5000	10,000

constant voltage power processing units (PPUs) affect the thrust-to-drag (T/D) ratio.

In this analysis, there are two constants. The coefficient of drag is 2.4, and the transparency of each AAIT grid is 90%. Changing these inputs does not require a new set of STK files; this saves much STK and AEPMPT run time. Each STK input file contains approximately 525,000 orbit propagation points. At each point, the AEPMPT calculates the performance parameters and averages these parameters per mission for ease of analysis. The code run time requires approximately 40 min for calling the IRI FORTRAN 77 scripts per mission and less than 2 min for performance calculations per configuration. This run time is found for a computer running Linux with an Intel Core 2 Quad Q9650 3.0 GHz processor and 3.0 GB of random-access memory.

The performance code simulates 72 different orbits (various altitudes, inclinations, and solar activity levels). The analysis of each mission adds 27 different cases by varying the spacecraft frontal area, AAIT grid area, and AAIT acceleration voltage. The total number of analyses is thus 1,944. The figures in this paper show performance results from selected conditions.

The output includes the thrust, drag, T/D ratio, and power at each propagation point in an orbit with each specific set of satellite and AAIT parameters. The code also calculates the averages of the thrust, drag, T/D ratio, and power over many orbits in the entire one year orbit duration; these averages provide a quick and useful analysis of how the AAIT performs through day-and-night and seasonal fluctuations since ion densities vary between day and night and throughout the year.

A. AAIT Performance Code and IRI Integration Verification

The verification of a properly working code is essential and is accomplished by analyzing the effects of transient conditions expected while in orbit. With regard to ion and neutral densities, the code should exhibit transient thrust and drag as the spacecraft orbits through sunlight and darkness. Figure 3 shows the AAIT thrust, total drag, and total T/D ratio at each orbital propagation point for the first three orbits (approximately 4.5 h) of a 400 km circular, equatorial orbit with mean solar activity, 1.5 m^2 satellite frontal area, 5 m^2 AAIT total grid area, and 5 kV acceleration voltage. Equations (1) and (3) show that, for a given AAIT acceleration voltage and transparency, the thrust is directly proportional to the mass flux of ions entering the AAIT open area. This confirms that, as the satellite orbits the Earth, the combined ion densities reach a minimum during darkness and a peak during sunlight. The drag shows very small changes compared to the thrust, which, from Eq. (4), is expected since STK shows that, at this altitude, the neutral density is much larger than the combined ion densities. Furthermore, the neutral density in STK is a strong function of the altitude, so we find that the neutral density is constant during the orbit as a function of time.

B. Thrust-to-Drag Ratio

The average T/D ratio is the average over the entire analysis duration of the ratio of the AAIT thrust in Eq. (1) and the drag from both the AAIT and satellite in Eq. (4). Figure 4 displays the average T/D ratio calculated with the AAIT performance code for altitudes between 300 and 1,000 km. This T/D ratio analysis is a function of the orbit altitude, AAIT grid area, and AAIT acceleration voltage with a constant mean solar activity level and a constant 1.5 m^2 spacecraft drag area. The T/D ratio increases as the altitude increases, when all other parameters are held constant, because the neutral number density (drag) decreases more relative to the ion number density decrease (thrust). The largest AAIT grid area and acceleration voltage of 10 m^2 and 10 kV, respectively, produce a larger T/D ratio than the other AAIT configurations at all altitudes. This is the expected result, as increases in both grid area and acceleration voltage increase thrust.

Figure 5 displays the average T/D ratio from the AEPMPT for altitudes between 300 and 1,000 km. This T/D ratio analysis is a function of the orbit altitude, orbit inclination, and solar activity level. In this study, the constants are a 1.5 m^2 spacecraft frontal area, 5 m^2 AAIT grid area, and 5 kV acceleration voltage. The T/D ratio retains the same trends with altitude as in Fig. 4, but now the effects of the orbit inclination and solar activity level manifest. We expect that equatorial orbits during maximum solar activity will produce the greatest T/D ratio, but each condition increases the thrust for a different reason. First, measurements show that lower latitudes contain the highest electron number density [4,13]. Since the IRI calculates an equivalent number of ions as electrons, the maximum thrust should occur at lower latitudes at which there exists a higher ion density. Second, higher solar activity typically indicates higher number densities of ions in the ionosphere [12]. Therefore, a maximum solar activity year should produce a higher thrust than the minimum or mean solar activity years.

Figure 5 shows clear distinctions in each set of parameters. As expected, higher solar activity and lower latitude orbits produce larger T/D ratio values. This figure also shows a clear distinction in that the minimum solar activity orbits remain at lower T/D ratio values than all of the mean solar activity orbits, which in turn are at lower T/D ratio values than the maximum solar activity orbits.

A standard criteria for defining the AAIT operational range can be a T/D ratio of one or greater. Many configurations of the AAIT and satellite frontal areas provide a T/D ratio greater than one at multiple altitudes, but the lower the altitude, the larger the required AAIT grid area and/or acceleration voltage. The T/D ratio first exceeds one at altitudes slightly greater than 400 km. A more accurate estimation of the altitude at which T/D ratio exceeds one is not possible from this set of simulations, as the interval between altitudes is 100 km. A finer altitude resolution will identify this limit but should be examined for specific missions. Approximately half of the considered simulations achieve a T/D ratio of one or greater by 500 km. At this altitude, a 5 m^2 AAIT grid area, or larger, and 5 kV acceleration voltage, or

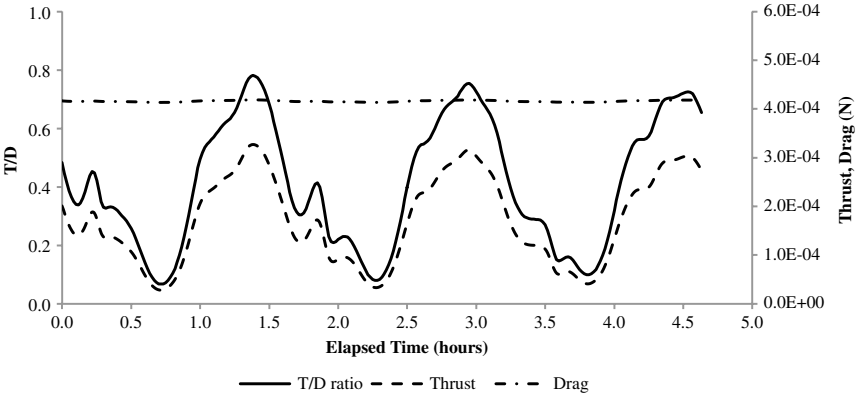

Fig. 3 AAIT thrust, total drag, and total T/D ratio for the first three orbits of a 400 km circular, equatorial orbit with mean solar activity, 1.5 m^2 satellite frontal area, 5 m^2 AAIT total grid area, and a 5 kV acceleration potential.

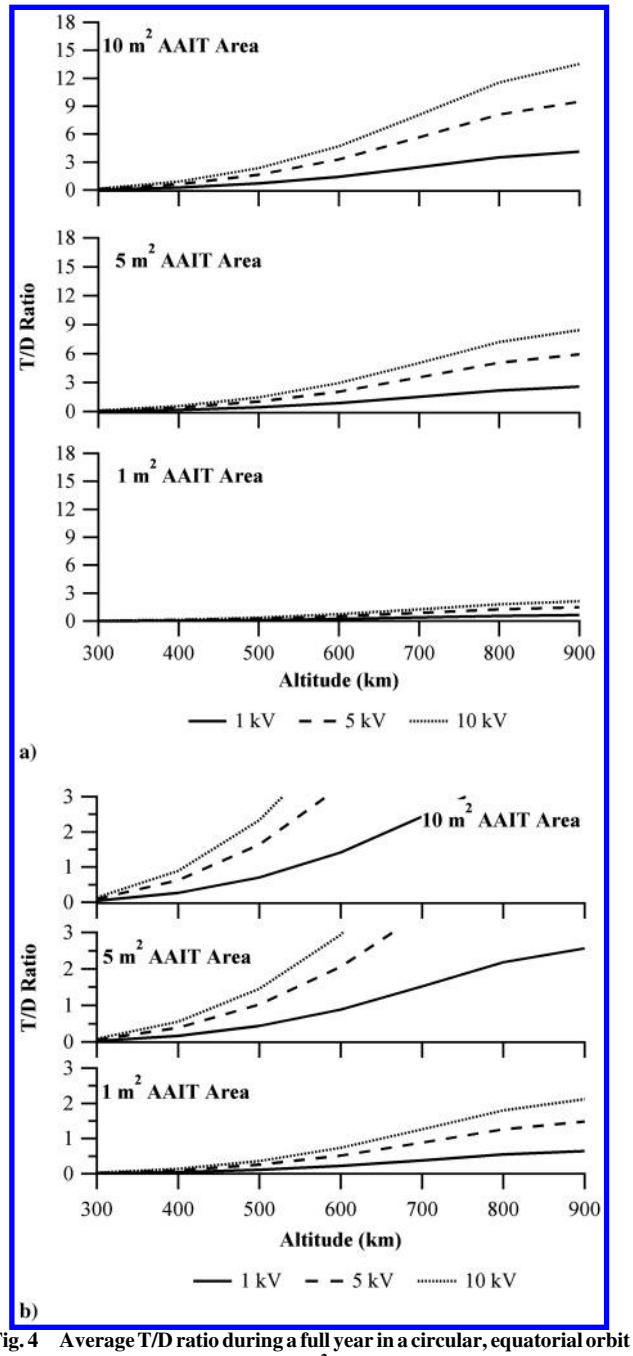

Fig. 4 Average T/D ratio during a full year in a circular, equatorial orbit with mean solar activity and a 1.5 m^2 spacecraft drag area. This figure shows a) the full range of T/D ratio and b) a subset of a) to identify the altitudes at which configurations achieve a T/D ratio of 1.

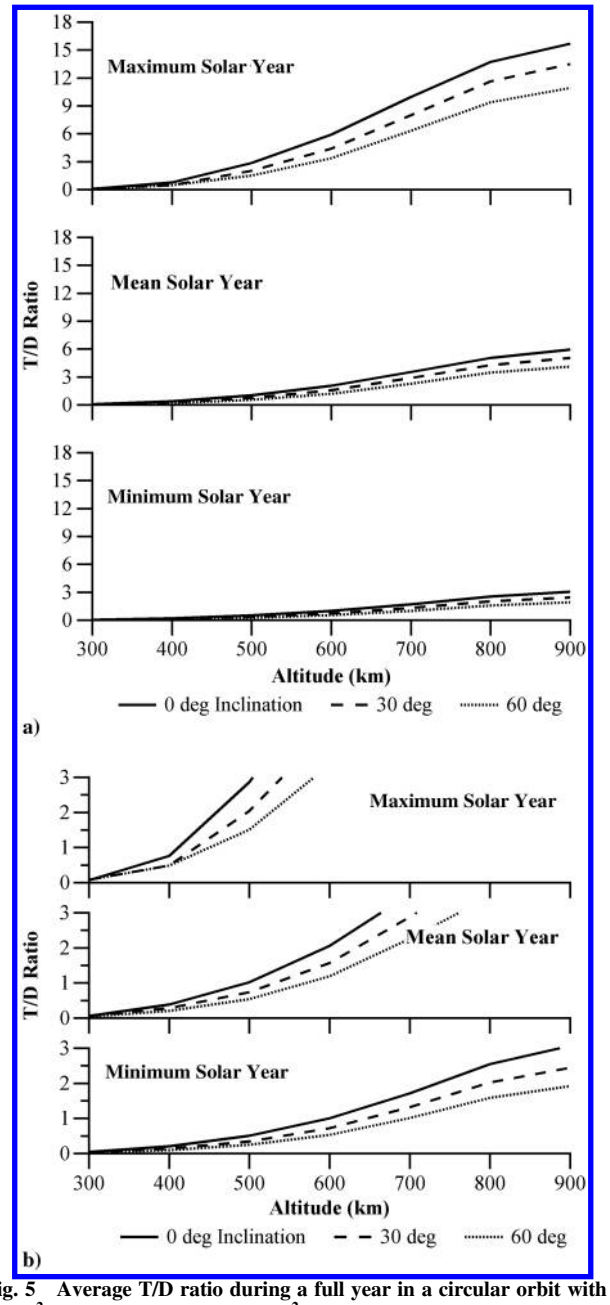

Fig. 5 Average T/D ratio during a full year in a circular orbit with a 1.5 m^2 spacecraft drag area, 5 m^2 AAIT area, and 5 kV acceleration voltage. This figure shows a) the full range of the T/D ratio and b) a subset of a) to identify the altitudes at which configurations achieve a T/D ratio of 1.

larger, with mean solar activity will achieve a T/D ratio greater than one. At the high end at 900 km, every configuration achieves a T/D ratio greater than one except the case of the 1 m^2 AAIT grid area and 1 kV acceleration voltage.

There also exist many configurations and altitudes at which the T/D ratio is less than one. The AAIT would benefit satellites in lower altitude orbits (300–500 km), in which the thrust does not completely compensate the drag by extending the satellite lifetime with the added benefit of no thruster propellant mass. With regard to spacecraft design, the T/D ratio values obtained from the AAIT analysis would reduce mission delta-v requirements by an equivalent percentage. For example, if the average T/D ratio is 0.8 then the mission Delta-V requirement would be reduced by 80%, on average, and a propulsive manuever would be required to make up for the remaining 20%, on average.

Although the T/D ratio was calculated up to 1000 km, it increases significantly above 900 km. At 1000 km, STK exports an atmospheric (neutral atom) density of 0 kg/km^3. This absence of atmospheric density results in extremely large values of the T/D ratio, between about 100 and 150. The code has been thoroughly examined to ensure that the extremely low STK atmospheric density is the reason for this large T/D ratio change. Truncating the T/D ratio values to those at 900 km in the T/D ratio figures allows the visibility of trends in the altitudes below 1000 km.

C. Power

Figure 6 displays the average AAIT power over the entire one year analysis duration as calculated with the AEPMPT. The code calculates power with Eq. (5) and includes jet power, from the AAIT plume; grid power, from ion strikes on the grids; and ionization power, from raising the potential of ions. Figure 6 shows the power of the AAIT at the same conditions as the simulations from Fig. 4. One

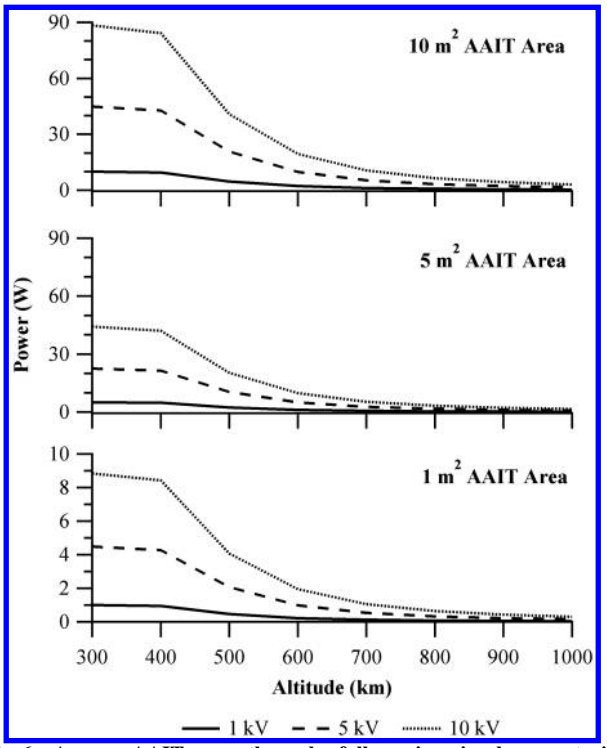

Fig. 6 Average AAIT power through a full year in a circular, equatorial orbit with mean solar activity and 1.5 m² spacecraft drag area.

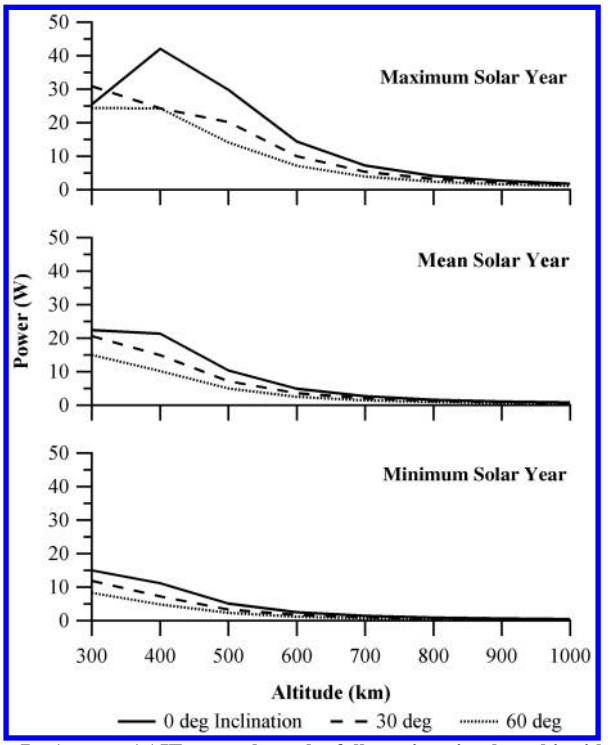

Fig. 7 Average AAIT power through a full year in a circular orbit with a 1.5 m² spacecraft drag area, 5 m² AAIT area, and 5 kV acceleration voltage.

can make a direct comparison of the T/D ratio and the associated AAIT power by referencing Figs. 4 and 6. The average power decreases with increases in altitude, contrary to the average T/D ratio, since power is a function of ion density and ion speed, both of which decrease as altitude increases. The average power also increases linearly with larger grid areas, due to the larger numbers of ions entering the AAIT, and larger acceleration voltages, due to the larger energy imparted to the incoming ions.

A close look at Fig. 6 shows that a number of simulated AAIT configurations appear to have identical power results during the same orbit simulation. The power results are, in fact, not equal but differ by less than 0.1%. Equations (6) and (7) give insight to this phenomenon and clarify as to why these different cases produce very similar results. The AAIT jet and grid power are functions of the incoming current density, but the reference areas and voltages differ considerably. The jet power is linearly proportional to the AAIT open area A_{open} and the acceleration voltage ΔV. The grid power is linearly proportional to the AAIT grid area A_{grid} and the screen grid voltage V_{screen}. The grid power in these simulations is orders of magnitude less than the jet power since the physical grid area is 10% of the total grid area and the ratio of screen voltage to acceleration voltage is much less than one. Therefore, cases in which the multiples are the same value, such as the 5 m^2 grid area with 1 kV acceleration voltage (5 $m^2 \cdot$ kV) and 1 m^2 grid area with 5 kV acceleration voltage (5 $m^2 \cdot$ kV), obtain very similar power results. This is a useful result, as it enables one to accurately estimate AAIT power requirements in the same orbital configuration for varying AAIT configurations.

Figure 7 displays the average AAIT power over the entire analysis duration as calculated in the AAIT performance code. Figure 7 is the power of the AAIT at the same conditions as the simulation from Fig. 5. One can make a direct comparison of the T/D ratio and the associated AAIT power by referencing these figures. As is shown in Fig. 7, the average power increases during higher solar activity, due to larger ion number densities, and lower orbit inclinations, due to larger ion densities near the equator than near the poles. The average power in a circular, equatorial orbit during maximum solar activity shows a sharp increase from 300 to 400 km. This rise occurs due to the ion number density outputs of the IRI code. Possible reasons for this include the model breakdown of ion densities at low latitudes and low altitudes, as is noted in published IRI papers; sensitive ion number densities at 400 km; or insensitive ion number densities at 300 km. Figure 7 gives some insight on the latter reasons, as it shows the average power on the same orbit at different solar activity levels. The power is generally higher at 300 km than 400 km, so, as the solar activity increases, the ion number density at 300 km may not change as considerably as the ion number density at altitudes of 400 km and higher.

The average ionization power estimated with the AEPMPT ranges between 1.1% and 14.3% of the total average AAIT power. These small percentages of the total AAIT power show that one can design and include an ion potential raising device while maintaining a low AAIT power, on average. Further, one can verify with Eqs. (6) and (8) that the ratio between these equations gives an order of magnitude maximum of 100 and an order of magnitude minimum of 10, and these values depend only upon the ionization energy, acceleration voltage, and ionization power loss factor. To maximize this ratio (and minimize the ionization power ratio of the total AAIT power), one would increase the acceleration voltage and minimize the power loss of the ion potential raising device.

IV. Conclusion

The Atmospheric EP Mission Performance Tool is an important tool that predicts the T/D ratio and power requirements of an atmospheric EP device in various orbits with multiple satellite frontal areas, grid areas, and acceleration voltages. More specifically, the AEPMPT has been created to integrate an electrostatic EP design that uses ambient atmosphere ions with an atmospheric model. This code can be modified to include any acceleration mechanism, an alternative orbit propagator, or a specific ion potential raising device.

The AEPMPT shows that larger AAIT grid areas, larger acceleration voltages, larger altitudes, and higher solar activity all help to increase the T/D ratio of a satellite using one or more AAITs. In general, as the altitude increases, the T/D ratio increases while the required power decreases. In this analysis, the T/D ratio first exceeds one between 400 and 500 km, but an exact number cannot be given because the resolution of altitudes is large. A finer altitude resolution should identify this limit but should be examined for specific missions. The conditions of a 500 km, 5 m^2 AAIT grid area, or larger, and 5 kV acceleration voltage, or larger, with mean solar activity will

achieve a T/D ratio greater than one. At 900 km, every configuration aside from the lowest AAIT grid area and acceleration voltage configuration achieves a T/D ratio greater than one.

Although this shows potentially useful AAIT performance, the satellite lifetime at these higher orbits is long enough to satisfy most missions without additional station keeping. The AAIT power less than 100 W at low altitudes, less than 400 km, will not pose a burden on satellite power systems that are capable of providing in excess of a few hundred Watts of bus power. If this is the case, satellites will not last indefinitely with T/D ratio values less than one but will be extended by months or years with the use of the AAIT. Additionally, the AAIT would be capable of accelerating deorbit of a spacecraft after mission completion. This may benefit scientific, military, and civilian needs as spacecraft continue to populate orbits around Earth.

References

[1] Dressler, G. A., "Spacecraft Propulsive Device Using Ambient Upper Atmospheric Constituents for Reaction Mass," *42nd Joint Propulsion Conference & Exhibit*, AIAA Paper 2006-4650, 2006.

[2] King, S. T., Walker, M. L. R., and Chianese, S. G., "Ambient Atmosphere Ion Thruster (AAIT) Proof-of-Concept Modeling," *47th Joint Propulsion Conference & Exhibit*, AIAA Paper 2011-6000, 2011.

[3] Goebel, D. M., and Katz, I., *Fundamentals of Electric Propulsion: Hall and Ion Thrusters*, Jet Propulsion Laboratories Space Science and Technology Series, Jet Propulsion Lab., California Inst. of Technology, Pasadena, CA, March 2008, pp. 91–103.

[4] Bilitza, D. (ed.), "International Reference Ionosphere 1990," NSSDC/WDC-A-R&S 90-22, NASA Goddard Space Flight Center, Greenbelt, MD, Nov. 1990.

[5] Bilitza, D., "International Reference Ionosphere 2000: Examples of Improvements and New Features," *Advances in Space Research*, Vol. 31, No. 3, 2003, pp. 757–767.
doi:10.1016/S0273-1177(03)00020-6

[6] Bilitza, D., and Reinisch, B., "International Reference Ionosphere 2007: Improvements and New Parameters," *Advances in Space Research*, Vol. 42, No. 4, 2008, pp. 599–609.
doi:10.1016/j.asr.2007.07.048

[7] Moe, K., and Moe, M. M., "Gas-Surface Interactions and Satellite Drag Coefficients," *Planetary and Space Science*, Vol. 53, No. 8, 2005, pp. 793–801.
doi:10.1016/j.pss.2005.03.005

[8] Vallado, D. A., and Finkleman, D., "Assessment of Satellite Drag and Atmospheric Density Modeling," *Astrodynamics Specialist Conference & Exhibit*, AIAA Paper 2008-6442, 2008.

[9] Lide, D. R. (ed.), *CRC Handbook of Chemistry and Physics*, CRC Press, Boca Raton, FL, 2009, Chap. 10.

[10] Kuo, S., Zhang, Z., Ross, S. K., Klemm, R. B., Johnson, R. D., III, Monks, P. S., Thorn, R. P., Jr., and Stief, L. J., "Discharge Flow-Photoionization Mass Spectrometric Study of HNO: Photoionization Efficiency Spectrum and Ionization Energy and Proton Affinity of NO," *Journal of Physical Chemistry A*, Vol. 101, No. 22, 1997, pp. 4035–4041.
doi:10.1021/jp9705941

[11] Samson, J. A. R., and Gardner, J. L., "On the Ionization Potential of Molecular Oxygen," NASA CR-142294, 1974.

[12] Moussas, X., Polygiannakis, J. M., Preka-Papadema, P., and Exarhos, G., "Solar Cycles: A Tutorial," *Advances in Space Research*, Vol. 35, No. 5, 2005, pp. 725–738.
doi:10.1016/j.asr.2005.03.148

[13] Rawer, K., Bilitza, D., and Gulyaeva, T. L., "New Formulas for the IRI Electron Density Profile in the Topside and Middle Ionosphere," *Advances in Space Research*, Vol. 5, No. 7, 1985, pp. 3–12.
doi:10.1016/0273-1177(85)90347-3

R. Sedwick
Associate Editor